E6 and E7 Oncoproteins Induce Distinct Patterns of Chromosomal Aneuploidy in Skin Tumors from Transgenic Mice

Anthony J. Schaeffer,[1] Marie Nguyen,[2] Amy Liem,[2] Denis Lee,[2] Cristina Montagna,[1] Paul F. Lambert,[2] Thomas Ried,[1] and Michael J. Difilippantonio[1]

[1]Genetics Branch, Center for Cancer Research, National Cancer Institute/NIH, Bethesda, Maryland; and [2]McArdle Laboratory for Cancer Research, University of Wisconsin Medical School, Madison, Wisconsin

ABSTRACT

Inactivation of the tumor suppressor genes *p53* and *Rb* are two of the most common genetic alterations in cancer cells. We use a mouse model to dissect the consequences of compromising the function of either of these genes on the maintenance of genomic stability. Thirteen cell lines established from skin tumors of mice expressing either the E6 or E7 oncoprotein of the human papillomavirus (HPV) type 16 under control of the keratin 14 promoter were analyzed by comparative genomic hybridization, spectral karyotyping and fluorescence *in situ* hybridization, reverse transcription-PCR, and mutation analysis. Deducing from the wealth of molecular cytogenetic data available from human cancers, we hypothesized that the more benign tumors in mice expressing E7 would be distinct from the more aggressive lesions in E6 transgenic mice. Tumorigenesis in E6-expressing mice required specifically the selection and maintenance of cells with extra copies of chromosome 6. Aneuploidy of chromosome 6 was independent of activating mutations in H-*ras* on chromosome 7. Expression of either E6 or E7 resulted in centrosome aberrations, indicating that each viral oncoprotein interferes independently with the centrosome cycle. Although centrosome aberrations are consistent with development of aneuploidy, no direct correlation was evident between the degree of aneuploidy and the percentage of cells with aberrant centrosomes. Our results show that although aneuploidy and centrosome aberrations are present in tumor cells from mice expressing either E6 or E7, tumorigenesis via E6 requires copy number increases of mouse chromosome 6, which is partially orthologous to human chromosome 3q, a region gained in HPV-associated carcinomas.

INTRODUCTION

The retinoblastoma susceptibility gene (*Rb*) and *p53* are tumor suppressor genes whose proper functioning is vital to maintaining genomic stability and normal cell growth and differentiation. Responding to extracellular and intracellular signals, *Rb* is responsible for the correct timing of the G1-S transition and for regulating the S, G2, and M phases of the cell cycle. Inactivation of Rb leads to genomic instability by impaired growth control, imprecise timing of DNA synthesis, and chromosome mis-segregation (1). As an integral member of the DNA damage control pathway, p53 functions in the recognition and repair of damaged DNA and in programmed cell death. The loss of wild-type p53 eliminates a major roadblock in tumorigenesis, allowing cells with damaged DNA to proceed through the cell cycle, thereby propagating genomically unstable progeny containing random mutations, gene amplifications, chromosomal rearrangements, and/or aneuploidy (2).

Unfaithful chromosome segregation during mitosis can lead to aneuploidy, a genetic defect observed consistently in tumor cells. Proper chromosome segregation depends on attachment of mitotic spindles to the kinetochore of each chromosome. The centrosome, responsible for nucleating and organizing mitotic spindles, is an essential component of this process (3). As such, the centrosome duplication cycle is synchronized with the cell division cycle, and uncoupling these cycles results in centrosome numbers above the normal 1–2 per cell. Increased centrosome numbers can lead to multipolar mitoses, mis-segregation of chromosomes, and genomic instability (4). Numerical and/or structural centrosome abnormalities have been reported in a variety of cancers, including breast cancer (5), colon cancer (6), pancreatic cancer (7), head and neck cancer (8), and human papillomavirus (HPV)-associated squamous cell carcinoma (9), and is observed in a variety of mouse models of human cancers (10–12).

The respective roles that p53 and Rb play in centrosome duplication are unclear. Duensing *et al.* (9) found that cells expressing a mutant E7 protein unable to inactivate Rb had threefold-less centrosome amplification than cells expressing an Rb-inactivating E7 protein. The E7 mutant was equivalent roughly with respect to centrosome amplification to the untransfected control, and thus their results linked Rb functionally to proper centrosome duplication. This is in contrast to other studies in which the absence or inhibition of Rb function had either no affect on centrosome number (8, 13) or depended on the mode of Rb inactivation (14). Likewise, there also has been debate as to whether centrosomes are affected by the absence of p53 function. Carroll *et al.* (8) and Fukusawa *et al.* (13) have shown that p53 deficiency induces directly increased centrosome numbers. In contrast, centrosome amplification was observed in epidermal tumors from mice expressing a mutant form of *p53* but not in *p53* knockout mice after treatment with 7,12-dimethylbenz(a)anthracene (DMBA) and 12-*O*-tetradecanoyl-phorbol-13-acetate (TPA) (15, 16). Thus, more investigation into the role of Rb and p53 with respect to centrosome amplification, chromosome instability, and tumorigenesis is warranted.

To address experimentally the independent effects of p53 and Rb inactivation with respect to centrosome abnormalities and genomic instability, we used a previously established mouse model of skin cancer (17). Our particular model system uses the human keratin 14 (K14) transcriptional promoter to express two HPV type 16 viral oncogenes, E6 and E7, in the basal epithelial cells of the epidermis. HPVs are DNA tumor viruses that cause benign tumors or warts in human skin. A subset of HPVs, including HPV types 16 and 18, are high-risk HPVs associated with cervical cancers (18, 19). In progressing from a low-grade squamous intraepithelial lesion to a high-grade squamous intraepithelial lesion, the high-risk HPV genomes are commonly integrated into the host's genome, and the E6 and E7 oncogenes become overexpressed (20). In binding to and degrading p53 and Rb, respectively, the E6 and E7 proteins confer transforming abilities to the cell, but their contributions to carcinogenesis are different. Molecular dissection of the respective pathways has shown specifically that the expression of E7 contributes primarily to early stages of carcinogenesis, leading to the formation of benign lesions. In contrast, E6 affects primarily later stages of carcinogenesis, leading to malignant conversion (20).

Previous observations of cervical (21), colorectal (22), breast (11), and head and neck (23) tumors have revealed specific patterns of

chromosomal gains and losses associated with distinct stages of tumorigenesis. Our model system is significant because we are able to correlate a lesion's phenotype with its genotype and thereby develop a map of chromosomal and genetic imbalances associated with K14E7 *versus* K14E6 tumors as they relate to the impairment of either Rb or p53 function, respectively. On the basis of observations in epithelial carcinogenesis, we hypothesize that few random chromosomal aberrations would be present in less severe lesions and that progression toward carcinoma and frank malignancy would correlate with the acquisition of additional specific chromosomal aberrations. Our investigation of genomic stability in this mouse model system also involved an assessment of whether Rb or p53 inactivation could lead to centrosome abnormalities, which still is a matter of controversy (8, 9, 13–16).

MATERIALS AND METHODS

Generation of K14E6 and K14E7 Mice. The generation of these transgenic mouse lines has been described previously (24, 25). A contiguous region of HPV type 16 genome from nucleotide 79–883 was inserted between the human K14 promoter and human K14 polyadenylation sequences. The line of K14E6 mice used in this study is #5737 (originally named K14E6E7TTL in Ref. 25). Approximately 15% of line 5737 K14E6 mice develop tumors spontaneously by 15 months (25). The line of K14E7 mice used in this study is #2304 (originally named K14E6TTLE7 in Ref. 24), of which ~10% develop spontaneous tumors by age 15 months. Spontaneously arising tumors were excised once they were >0.5 cm but <1 cm in diameter. The age of the mice at the time of tumor excision was 8–12 months.

Skin Tumor Induction with DMBA and TPA. Eight-week-old mice were treated as described previously (20). The back was shaved, and the carcinogenic initiator DMBA dissolved in acetone was applied. After 1.5 weeks, 2.5 μg of a carcinogenic promoter TPA dissolved in acetone were applied twice weekly for 20 weeks. Mice were monitored weekly for skin tumors and were killed when the tumors reached 5 mm in diameter or when the tumors became ulcerated. When a mouse was killed, a portion of the tumor was fixed in 10% buffered formalin or frozen at −80°C for histologic analysis. Another portion of the tumor was placed in DMEM medium containing penicillin and streptomycin and was used to generate cell lines. Tumors were excised at age 7–9 months, with time of onset of malignancy first observed 3–6 weeks before tumor excision. For humane reasons, no more than one carcinoma was allowed to develop per animal before killing.

Generation of K14E6 and K14E7 Tumor Cell Lines. Keratinocyte cell lines were derived from tumors of six K14E6 mice and seven K14E7 mice. The tumors were washed twice in PBS, minced with scalpel blades, and dissociated in 0.125% trypsin-EDTA (Life Technologies, Rockville, MD) for 7 min at 37°C after a 1-h incubation at 4°C. The reaction was terminated with 3 ml of fetal bovine serum (FBS), and the cells were collected and plated on collagen IV-coated flasks (Becton-Dickinson, Bedford, MA) in modified, Ca^{2+}-free Eagle's MEM with 8% FBS containing 0.5 mM Ca^{2+} and enhanced with 100 ng/ml mouse epidermal growth factor, 250 ng/ml fungizone antimycotic, and penicillin-streptomycin, 60 units/ml and 60 μg/ml, respectively (Life Technologies). After 24 h, the medium was changed to Ca^{2+}-free Eagle's MEM with 8% FBS containing 0.05 mM Ca^{2+} and enhanced as described previously. After the second passage, the cells were plated for 24 h in unenhanced Eagle's MEM and 8% FBS with 0.5 mM Ca^{2+} to facilitate attachment and maintained in unenhanced Eagle's MEM and 8% FBS with 0.05 mM Ca^{2+}. Calcium concentrations were chosen to maintain cells in their undifferentiated proliferating state as described previously (26). The cultures were cleared of contaminating fibroblasts by differential trypsinization.

Cytogenetic Analysis. Metaphase chromosomes for spectral karyotyping (SKY) were prepared after exposure to colcemid arrest (1–3 h; 100 μg/ml) from all of the tumor cells at passages 6–9 and again from Tm5 and Tm9 at passage 40. The cells were lysed in hypotonic solution (0.075 M KCl), and the nuclei were fixed in methanol and acetic acid (3:1). SKY was performed as described (27, 28). Six to 12 metaphases were analyzed for each tumor, and karyotypes were defined using the nomenclature rules from the International Committee on Standardized Genetic Nomenclature for Mice (29).

Comparative genomic hybridization was performed as described (11, 30). Quantitative fluorescence imaging and comparative genomic hybridization (CGH) analysis was performed using Leica CW4000CGH software (Leica Imaging Systems, Cambridge, United Kingdom).

Metaphase chromosomes for fluorescence *in situ* hybridization were prepared as described previously. A mouse chromosome 6 painting probe was prepared from a flow-sorted chromosome preparation and labeled directly with spectrum orange by degenerate oligonucleotide primed PCR (31). A plasmid containing the mouse K-*ras* gene was labeled with biotin-11-dUTP and detected with avidin-FITC (32).

Instability Calculation. The copy number of each chromosome was assessed by SKY analysis of metaphase spreads, and the modal value (*i.e.,* the most frequently observed copy number) was identified for each chromosome. The total number of copy number changes (*i.e.,* gains and losses relative to the modal value for each chromosome) for each tumor line then was divided by the number of metaphases analyzed ($CIX = \Sigma|chromosome\ count_n − mode_n| / cell\ number$). This value, referred to as the chromosome instability index (CIX), is a measure of the amount of karyotypic variability observed in each tumor.

H-*ras* Mutational Analysis. H-*ras* mutations at the second position of codon 61 in all of the skin tumors were analyzed by PCR and RFLP as described previously (20). DNA fragments encompassing codon 61 (CAA) were amplified via PCR from tumor-derived DNA using the primer pair 5′-CTCCTACCGGAAACAGGTGGTC and 5′-GCTAGCCATAGGTGGCT-CACC. The PCR product then was digested with restriction enzymes *Xba*I, *Bsmp*HI, or *Tag*I to detect CAA to CTA, CAA to CAT, or CAA to GAA mutations. PCR products digested with these enzymes were run on 3% metaphor agarose gels and examined visually by ethidium bromide staining. Sequencing of the minus strand of the PCR products was performed to confirm the gel analysis of codon 61 and to inspect for mutations at codon 12/13 (GGA/GGC).

Isolation of Total RNA and Quantitative PCR for H-*ras* and K-*ras*. RNA was isolated from two independent cultures of three K14E7 (Tm2, Tm14, and Tm17) and three K14E6 (Tm12, Tm27, and Tm51) tumors following standard TRIzol procedures. The purified RNA from replicate cultures then was pooled in an attempt to reduce tissue culture condition-related artifacts (*i.e.,* cell confluency at time of harvest, age of medium, time since previous trypsination, and so on).

The Taq-Man assay was performed on 2 μg total RNA. Primer sequences and probes were as follows: H-*ras* (codons 128–149) forward (5′-GGCAG-GCCCAGGACC TT-3′), reverse (5′-CCGGGTCTTGGCTGATGTT-3′); K-*ras* (codons 117–141) forward (5′-AAGATGTGCCTATGGTCCTGG-TAGGG-3′), reverse (5′-GAACGGA ATCCCGTAACTCCTTGCT-3′); and glyceraldehyde-3-phosphate dehydrogenase (codons 132–166) forward (5′-CCCCCAA TGTGTCCGTCGTG-3′), reverse (5′-TGGGCCCTCAGATGC-CTGCT-3′). The H-*ras* (5′-ATGGCATCCCCTACATTGAA-3′) and K-*ras* (5′-CACGAAACAGGCTCAGGAGT-3′) probes were labeled with FAM, and the glyceraldehyde-3-phosphate dehydrogenase probe (5′-TGGAGAAACCT-GCCAAGTATG-3′) was labeled with MAX. The PCR conditions were 50°C for 2 min, 95°C for 10 min, 95°C for 15 s, and 60°C for 1 min for 40 cycles.

Immunofluorescence. Immunocytochemistry and centrosome enumeration were performed as described previously (6). Two observers evaluated at least 500 interphase and 50 metaphase nuclei for centrosome number and structure. A control group of primary keratinocytes was isolated from normal FVB/N mice and cultured in low Ca^{2+} (0.05 mM) Eagle's MEM as described previously for the tumor cells to avoid differentiation. After 1 week in culture, the cells were plated in chamber slides, and interphase cells were analyzed for centrosome aberrations.

RESULTS

Generation of K14E7 and K14E6 Tumor Cell Lines. To identify the consequences of inactivation of either *p53* or *Rb* tumor suppressor genes on genomic stability, we analyzed cell lines established from six K14E6 and seven K14E7 primary carcinomas. The incidence of spontaneous skin tumor formation in the K14E7 and K14E6 transgenic lines used in this study is 10% and 15%, respectively, by age 15 months (24, 25). To increase the number of tumor samples available for analysis, we also induced tumors with the carcinogenic initiator

DMBA, followed by the carcinogenic promoter TPA (see "Materials and Methods"). Of the tumors isolated, six spontaneously occurring tumors and seven tumors from chemically treated mice were established successfully in tissue culture once it was determined that plating in culture dishes coated with collagen IV was essential to their survival. To maintain the tumor keratinocytes in their undifferentiated proliferating state, the cultured cells were grown in medium containing a calcium concentration of 0.05 mM (low calcium) (26). Although the morphologic appearance of the cells was consistent with keratinocyte cell lines studied previously, the predominance of keratinocytes in each tumor line was verified by immunocytochemical analysis with an antibody-recognizing mouse K14. Because the human K14 promotor drives expression of the E6 and E7 transgenes, only those cells transcribing the endogenous K14 gene would be expected to express the viral oncogenes. Our immunocytochemical assessment revealed that at least 95% of the cells in each established tumor line expressed K14 (see Fig. 1 for example of K14 staining).

SKY Analysis Reveals a Consistent Chromosomal Gain in Tumors from E6, but Not E7, Mice. In our mouse model system, E7 and E6 oncoproteins contribute differently to tumorigenesis (20). Molecular dissection of the respective pathways has shown that the inactivation of Rb via expression of E7 contributes primarily at early stages of carcinogenesis, leading to the formation of benign lesions. p53 inactivation by E6, in contrast, affects primarily later stages of carcinogenesis, resulting in malignant carcinomas (25). We applied SKY and CGH to establish a map of chromosomal aberrations and genomic imbalances associated with K14E7 *versus* K14E6 carcinomas.

Karyotype analysis was performed on short-term cultures from three spontaneous and four chemically induced K14E7 lesions (Table 1). Although occasional structural aberrations were observed, the predominant karyotypic changes detected were numeric chromosomal aberrations (chromosomal aneuploidies). For example, T14 carried gains of chromosomes 1 and 16; T9 had a deletion of chromosome 2 and loss of chromosome 7 together with a gain of chromosome 18;
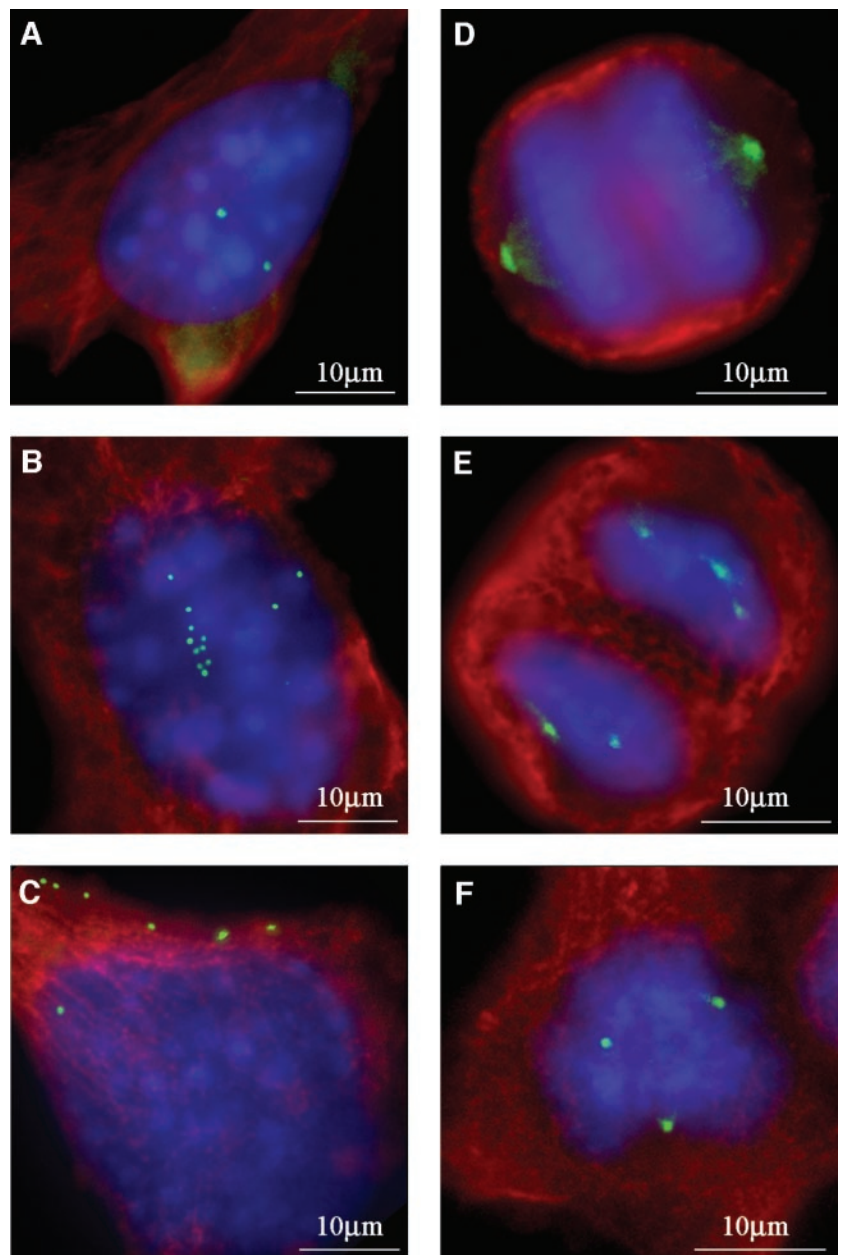

Fig. 1. Representative images of γ-tubulin (centrosome) and human keratin 14 (cytokeratin-14) staining. Normal interphase and mitotic cells are shown in (*A*) and (*D*), respectively. Some cells maintain the perinuclear localization of their supernumerary centrosomes (*B*), whereas they are no longer located near the nuclear membrane in other cells, but elsewhere within the cytoplasm, and are referred to as displaced (*C*). Despite the presence of extra γ-tubulin structures, bipolar mitosis sometimes was observed (*E*). The deleterious consequence of supernumerary centrosomes functionally capable of nucleating mitotic spindles is visualized easily in a multipolar mitosis (*F*).

Table 1 *Tumors isolated from K14E6 and K14E7 transgenic mice*

Indicated are the clonal genomic alterations detected by spectral karyotyping (SKY) and comparative genomic hybridization (CGH) and the H-*ras* codon 61 mutational status (wild-type, CAA at both loci; +/−, CAA at one locus and CTA at the other; −/−, CTA at both loci). Also presented is the histology of the tumor and whether it was spontaneous or chemically induced.

Tumor	Genotype	H-*ras* mutation[a]	CGH gains and losses	Histology	Mouse treatment
5	K14E6	WT/WT	+6, +10	Carcinoma	None
12	K14E6	n.d./(+/−)	+6, +10	Carcinoma grade I	None
27	K14E6	WT/(−/−)	+6	Days w/carcinoma grade I foci	DMBA + TPA[b]
41	K14E6	WT/WT	+1, −3, −4, +6, +10, +X	Carcinoma grade I	DMBA + TPA[c]
49	K14E6	WT/WT	+6, +10	Days w/carcinoma grade II foci	DMBA + TPA[c]
51	K14E6	WT/(−/−)	Dup 4(B), +6	Carcinoma grade I w/carcinoma grade II foci	DMBA + TPA[b]
1	K14E7	n.d./WT	None	Sarcoma	None
2	K14E7	WT/WT	None	Carcinoma grade I	None
6	K14E7	n.d./WT	None	Fibrosarcoma	None
9	K14E7	WT/WT	Del 2(C–E), −7, +18	Mammary carcinoma	None
14	K14E7	WT/WT	+1, +16	Carcinoma grade I and II	DMBA + TPA[b]
17	K14E7	WT/WT	+6	Carcinoma grade I	DMBA + TPA[b]
22	K14E7	n.d./(−/−)	None	NA	DMBA + TPA[b]

[a] Codon 12/13 and codon 61, respectively. WT, wild-type; +/−, heterozygous; −/−, homozygous mutant; n.d., not determined.
[b] 0.05 μM DMBA. DMBA, 7,12-dimenthylbenz(*a*)anthracene; TPA, 12-*O*-tetradecanoylphorbol-13-acetate.
[c] 0.01 μM DMBA.

and T17 displayed a gain of the entire chromosome 6 (Table 1). We did not observe any common aneuploidies between tumors from the K14E7 mice. Significantly, no differences were found between karyotypes from chemically induced *versus* spontaneously occurring tumors, thereby justifying the inclusion of samples from chemically induced tumors in our study.

In contrast to the K14E7 tumors, we detected consistent, nonrandom chromosomal gains in the K14E6 tumors. SKY analysis was performed on early passage specimens from two spontaneous and four chemically induced K14E6 tumors (Table 1). Similar to the K14E7 karyotypes, the predominant aberrations detected were chromosomal aneuploidies with few structural aberrations. Unlike the K14E7 karyotypes, however, all of the six K14E6 tumors analyzed revealed a consistent whole chromosome 6 gain (see Fig. 2 for representative karyotype). Furthermore, four of the six tumors (T5, T12, T41, and T49) exhibited additional gains of chromosome 10, a result that was later verified by CGH. Trisomy for chromosomes 6 and 10 were found in spontaneous (Tm5 and T12) and chemically induced (Tm41 and

Tm49) tumors, again supporting the notion that chemical induction of tumors does not modify the cytogenetic profile. In addition, T41 displayed loss of chromosomes 3 and 4, and T51 contained a duplicated region on chromosome 4. Complete karyotypes and accompanying CGH data can be found at the web site http://www.ncbi.nlm.nih.gov/sky/skyweb.cgi.

In summary, tumors derived from E6 and E7 transgenic mice demonstrated aneuploidy, the degree of which varied from tumor to tumor. However, there was a strong selection for the acquisition and maintenance of a specific chromosomal aneuploidy in the E6 transgenic mouse tumors. Therefore, we conclude that some gene or genes on chromosome 6 provide a sufficient advantage to the growth and/or survival of mouse skin epithelial cells expressing the HPV-E6 oncoprotein.

CGH Results Show No Significant Aberrations in K14E7 Tumors and Verify the Trisomy 6 in K14E6 Tumors. Although our analysis at the single-cell level by SKY did not reveal any significant patterns among the seven E7 cell lines, we used CGH, which samples
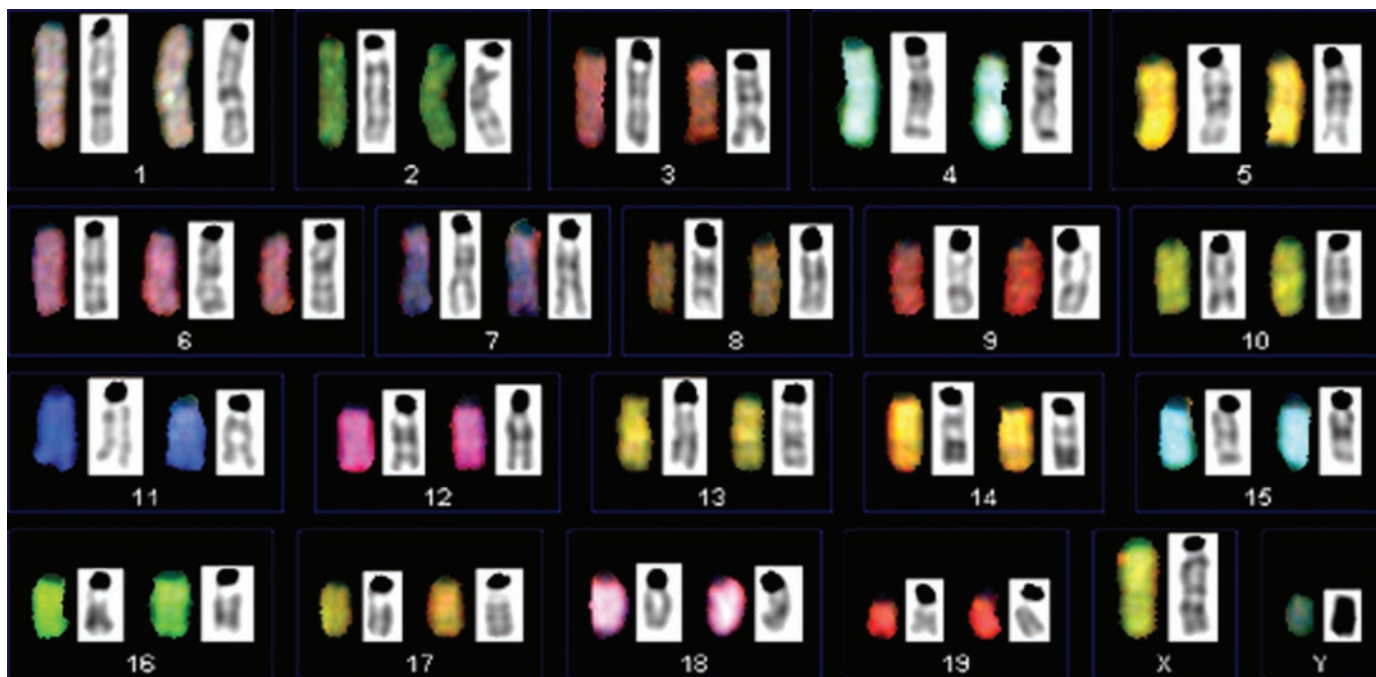

Fig. 2. Representative karyotype of E6 tumor cell lines. Spectral karyotyping and 4′,6-diamidino-2-phenylindole staining of Tm 5 is shown. Trisomy 6 was observed in all of the tumors from keratin 14 E6 mice regardless of treatment. The karyotype of this tumor (Tm5) is 41,XY,+6.

Fig. 3. Comparative genomic hybridization summary data. A bar to the right of a chromosome in the ideograms indicates a gain, and bars to the left represent a loss of genetic material. *A,* summary data from seven keratin 14 (K14) E7 cell lines (Tm9, red; Tm14, dark blue; and Tm17, orange). *B,* summary data from six K14E6 cell lines (Tm5, orange; Tm12, light blue; Tm27, dark blue; Tm41, green; Tm49, red; and Tm51, purple). E6 tumors display clear and consistent gains of chromosome 6 and chromosome 10, whereas E7 tumors show no consistent gain or loss of genetic material.
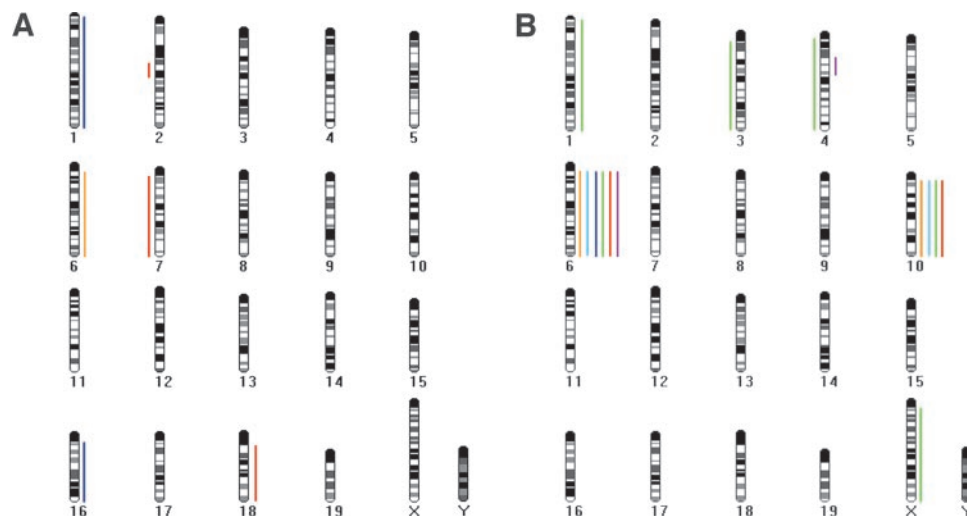
the entire cell population, to investigate whether there were other copy number changes. The CGH results verified the copy number changes and the consequences of structural alterations with respect to genomic imbalances identified previously by SKY and additionally enabled us to identify the deleted portion of chromosome 2 in Tm9 as bands C2-E2. As the E7 CGH summary data indicate (Fig. 3*A*), despite random chromosomal aneuploidies in individual tumors, the E7-induced tumors as a whole do not possess any specific chromosomal copy number aberrations.

Similarly, CGH data from the six E6 tumors is consistent with the chromosomal aneuploidies and structural aberrations identified by SKY. Most importantly, a gain of chromosome 6 was observed consistently in every E6 tumor. The E6 CGH summary data (Fig. 3*B*) additionally enhanced our analysis of E6 tumors by identifying additional chromosomal copy number changes not revealed in the SKY analysis. Although gains of chromosome 10 appeared in fewer than half of the cells examined by SKY from Tm5, Tm12, Tm41, and Tm49, an additional copy of this chromosome in the CGH profiles confirmed clearly and unambiguously the gain of chromosome 10 in the majority of cells in the population. In Tm41, CGH also detected a gain of chromosomes 1 and X in addition to the already identified loss of chromosomes 3 and 4. Finally, we were able to identify the region amplified in Tm51 as band 4B.

Gain of Chromosome 6 Correlates with Increased K-*ras* Gene Copy Number. The K-*ras* oncogene, located in the distal (telomeric) region of mouse chromosome 6, is amplified in many murine and human tumors. Therefore, we suspected that the recurrent gain of chromosome 6 observed by SKY and CGH in the tumors derived from K14E6 transgenic mice was the result of selective pressure to acquire additional copies of the K-*ras* gene. Therefore, we performed fluorescence *in situ* hybridization analysis on metaphase and interphase tumor cells using a chromosome 6-specific painting probe in conjunction with a differentially labeled probe for the K-*ras* gene. All of the additional copies of chromosome 6 contained the K-*ras* oncogene. Thus, a gain of chromosome 6 resulted directly in an increased number of K-*ras* genes in all of the K14E6 tumors and in one K14E7 tumor (Tm17).

H-*ras* Activating Mutations Do Not Correlate with E6/E7 Transgenes or Method of Induction. Although we found previously no H-*ras* mutations at either codon 12/13 or codon 61 in 24 of 24 spontaneous K14E6 tumors, we wanted to look at the tumors derived specifically for this study to determine if any correlations could be made with the mutational status of H-*ras* and the specific aneuploidies

we observe in the tumors (25). Restriction digest analysis and sequencing of codon 61-specific PCR products revealed the presence of A→T transversions in four of the tumors (Table 1; Fig. 4). Homozygous mutations were limited to tumors from those mice exposed to DMBA and TPA, in agreement with previous studies (20, 25, 33, 34). Two tumors (Tm27 and Tm51) were from E6 transgenic mice, and one tumor (Tm22) was from an E7 transgenic mouse. Not all of the chemically induced tumors carried H-*ras* mutations, regardless of the dosage. One spontaneously formed E6 tumor (Tm12) was heterozygous for the codon 61 A→T transversion, indicating that H-*ras* mutations can occur in the absence of chemical mutagenesis. No mutations in codon 12/13 were found in the 11 PCR products from which sequence information was obtainable.

K-*ras* Expression Levels Are Not Altered in Tumors with a Chromosome 6 Gain; However, H-*ras* Expression Is Reduced in Tumors with Activating Mutations. We observed that the K14E6 tumors generally grew faster than the K14E7 tumors, implying that these cells had a shorter cell division time. This observation would be
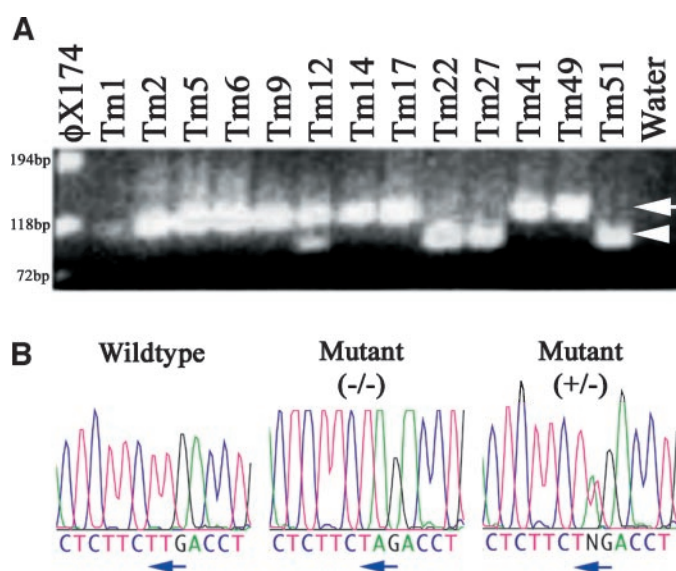

Fig. 4. H-*ras* mutational analysis. *A,* the results of restriction digest analysis of codon 61-specific PCR products. Indicated are bands representing the wild-type (←) and A→T transversion (▷). *B,* examples of results from the sequence analysis used to confirm the restriction digest results. The complimentary strand of the H-*ras* gene was sequenced; ← indicates the orientation of codon 61 (wild-type, CAA; mutant, CTA).

in agreement with the observed increase in K-*ras* gene copy number and potential overexpression of the oncoprotein. To test this hypothesis, quantitative real-time PCR was performed on total RNA isolated from three K14E6 (Tm12, Tm27, and Tm51) and three K14E7 (Tm2, Tm14, and Tm17) tumor cell lines. Our analysis did not indicate any statistically significant difference in the expression levels of K-*ras* between those tumors with additional copies of chromosome 6 (Tm12, Tm17, Tm27, and Tm51) and those without (Tm2 and Tm14) (Fig. 5; gray bars). However, there appeared to be a general trend that expression levels of K-*ras* relative to the glyceraldehyde-3-phosphate dehydrogenase control were lower typically in the K14E6 tumors. A similar analysis was performed for the H-*ras* oncogene located on mouse chromosome 7. We observed that the expression levels were lower for those cell lines with homozygous H-*ras*-activating mutations (Tm27 and Tm51) compared with those that were either wild-type at both alleles (Tm2, Tm14, and Tm17) or heterozygous mutants (Tm12; Fig. 5; black bars).

Chromosome Instability and Centrosome Abnormalities Are Present in E7 and E6 Tumors. The amount of chromosome instability in the tumors was based on an analysis of the chromosome content in numerous metaphases from each tumor sample and calculated as described in "Material and Methods." Some of the E7 tumors were relatively stable, averaging fewer than three changes in chromosome copy number per cell (Fig. 6*A*; Tm1, Tm9, Tm17, and Tm22). However, mitotic events in others tumors were rather catastrophic, averaging as many as 10 changes in chromosome copy number per cell (Fig. 6*A*; Tm2, Tm6, and Tm14). The K14E7 tumors as a group had an average CIX of 4.0, thus defining chromosome instability as a general feature of these E7-induced tumors. Tumors from K14E6 transgenic mice also had a variation in CIX with average values ranging from fewer than 1 (Tm 5) to as many as 10 changes per cell (Tm 49), with no significant differences observed between spontaneous and chemically induced tumors. As a group, the K14E6 tumors had an average CIX of 3.7, similar to that observed for the K14E7 tumors. Thus, the level of chromosome segregation errors was not appreciably different between tumors derived from K14E6 or K14E7 transgenic mice.

To understand how chromosome instability would affect the genome of these tumors after long periods in culture, karyotype analysis also was performed on late passage (passage 40) samples from two spontaneously formed E6 (Tm5*) and E7 (Tm9*) tumors. The chromosome deletions and numeric changes identified in the early-passage karyotypes also were present after prolonged passage, implying a selective pressure to maintain these specific genomic alterations. As a consequence of the genomic instability, however, both tumors acquired additional structural and numeric aberrations. As such, the CIX for both tumor cell lines increased slightly after prolonged passage
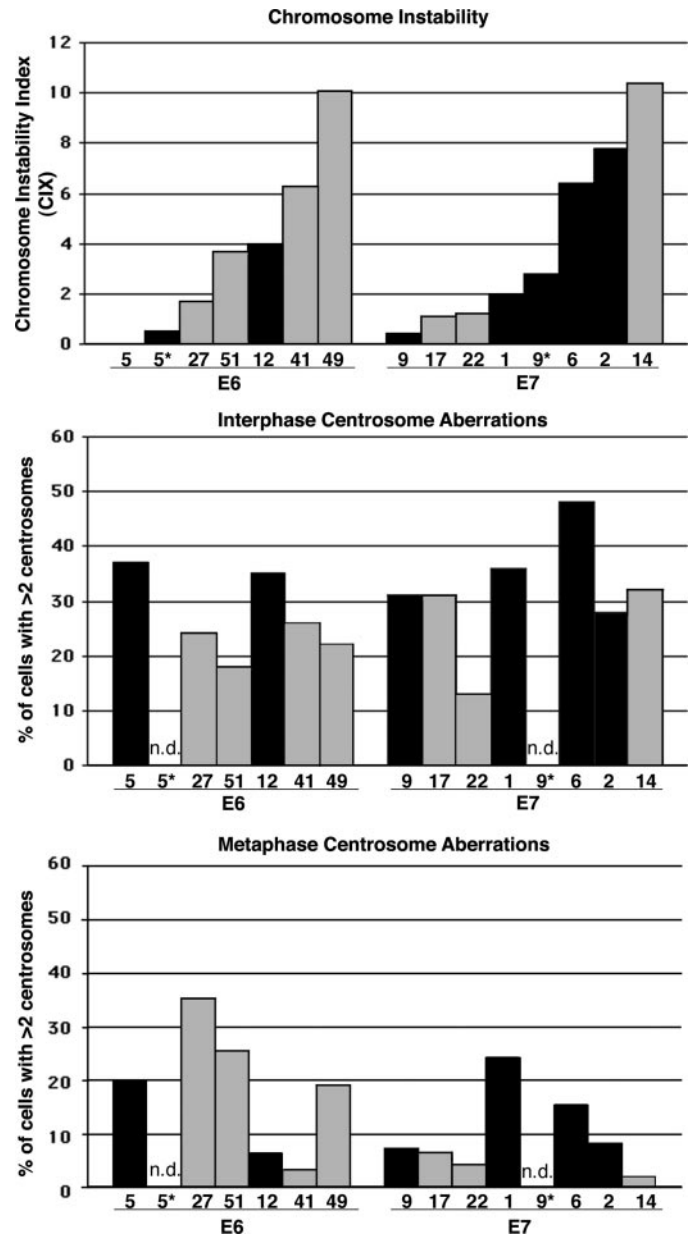

Fig. 6. Chromosome instability and centrosome aberrations. *A,* the tumors are organized based on their origin from keratin 14 (K14) E6 or K14E7 transgenic mice. Within each category, the tumors are arranged by increasing instability for visual simplicity. Black bars represent spontaneous tumors, and the gray bars represent those that were chemically induced. *Late passage tumors. The percentage of cells containing more than two centrosomes was determined for 500 interphase (*B*) and 50 mitotic (*C*) cells.

(0.0 and 0.4 at passage 6 *versus* 0.5 and 2.8 at passage 40 for Tm5* and Tm9*, respectively).

Most of the tumors, whether they occurred because of inhibition of Rb or p53 function, contained predominantly numeric chromosome aberrations, a finding consistent with a compromise in chromosome segregation fidelity during mitosis. Attachment of mitotic spindles to the kinetochore of each chromosome is essential for correct segregation during mitosis, and it is the role of the centrosome to nucleate and organize these structures (3). Therefore, we used an antibody against γ-tubulin, a protein that is concentrated in the centrosome during all stages of the cell cycle, to investigate whether abnormalities in centrosome number or function could account for the chromosomal aneuploidies we observed in the E7 and E6 tumors. Although we found many interphase cells with normal (1–2) centrosome numbers
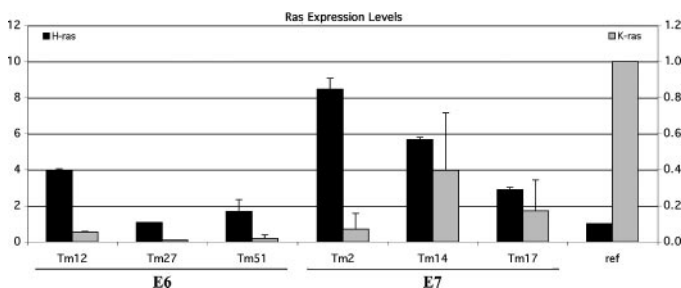

Fig. 5. *Ras* expression levels. RNA transcript levels of H-*ras* (black bars) and K-*ras* (gray bars) have been normalized to those observed in normal mouse skin keratinocytes. Tm12 and Tm2 are spontaneous tumors, whereas Tm27, Tm51, Tm14, and Tm17 were chemically induced. All three E6 tumors and one E7 tumor (Tm17) have increased copies of chromosome 6. All three E7 tumors are homozygous wild-type for H-*ras*; Tm12 is heterozygous; and Tm27 and Tm51 have homozygous-activating mutations.

(Fig. 1*A*), a significant proportion of cells also displayed an increased number of centrosomes. In some instances, cells managed to maintain the normal juxtaposition of these supernumerary structures to the nuclear membrane (Fig. 1*B*), whereas in other cells, some of the centrosomes were no longer located perinuclearly (Fig. 1*C*). Between 13% and 48% of E7 interphase cells displayed centrosome abnormalities compared with E6 tumors, in which abnormal centrosomes were observed in 18–37% of interphase cells (Fig. 6*B*). In undifferentiated mouse keratinocytes isolated directly from the skin of normal mice, we observed no more than 6% of interphase cells with centrosome aberrations.[3]

To determine if these supernumerary centrosomes had consequences during nuclear division, we also analyzed cells in the process of segregating their genome. In addition to cells containing two centrosomes and undergoing normal bipolar mitoses (Fig. 1*D*), we observed some cells with bipolar chromosome segregation but an increased number of centrosomes (Fig. 1*E*). Despite the bipolar nature of these cell divisions, however, one can neither assess the fidelity with which the genome is being partitioned to the daughter cells nor whether the supernumerary centrosomes are contributing to unequal chromosome segregation. This is not the case for the third subpopulation of cells observed, in which nucleation of mitotic spindles from more than two centrosomes resulted in the division of chromosomes in more than two directions, thereby increasing the likelihood that the resulting daughter cells, if viable, would be extremely aneuploid (Fig. 1*F*). Between 2% and 22% of E7 cells and between 3% and 35% of E6 cells displayed abnormal mitoses attributed directly to centrosome amplification (Fig. 6*C*).

DISCUSSION

The tumor-promoting HPV contains at least two genes, E6 and E7, which encode for proteins that interfere with cell-cycle regulation. E7 disrupts the cell cycle via its direct binding to Rb and other members of the retinoblastoma family (p107 and p130) [Refs. 33–36] and the cell-cycle regulatory proteins p21 (37–39) and p27 (40). The most prominent role of E6 involves the degradation of p53 via the ubiquitin pathway, thus impairing the ability of cells to either arrest the cell cycle or enter the apoptotic pathway in response to DNA damage. This action has been demonstrated to allow the progression of benign tumors to carcinomas. Transgenic mice expressing the *E6* and/or *E7* genes under keratin promoters develop skin papillomas, which, more frequently in the case of the former, progress into carcinomas (20, 24, 25, 43). We were interested in identifying whether these processes involved alteration of the genome through chromosome mis-segregation and, more importantly, whether such changes could distinguish the different tumorigenic pathways caused by each protein.

Tumors induced via chemical carcinogens, specifically the promoting agent DMBA followed by the initiator TPA, result in mutations in codons 12/13 and 61 of the H-*ras* proto-oncogene. Because these genetic modifications occur early during the formation of papillomas, they are considered generally to be causative events (41, 42). Similar mutations have been observed in tumors from transgenic mice expressing the HPV-18 *E6* and *E7* genes under control of the keratin 1 promoter (43). Expression of an activated form of H-*ras* is sufficient as an initiating agent in the formation of skin papillomas (44–46). Our mutational analysis, despite the presence of H-*ras* codon 61 mutations in four of the tumors, failed to reveal any unique correlation with expression of either the K14E6 (Tm12, Tm27, and Tm51) or K14E7 (Tm22) transgene. Although homozygosity for the activating codon 61 A→T transversion was observed only in tumors from mice

exposed to DMBA and TPA, not all of the chemically induced tumors contained mutations in H-*ras*. Additionally, none of the analyzed tumors contained mutations at codon 12/13. On the basis of previous reports, it is highly likely that mitotic recombination resulting in loss of heterozygosity was responsible for the observed allelic imbalances of the normal H-*ras* gene (47–50).

Copy number gains of chromosome 7, where the H-*ras* gene is located, have been observed in some instances to be concurrent with H-*ras* mutations (48). A gain of chromosome 7 was not seen in any of the K14E6 or K14E7 tumors, but rather a loss in one spontaneous K14E7 tumor by SKY and CGH (Tm9) and in one chemically induced K14E7 tumor by SKY only, and this was on a tetraploid background (Tm14). However, we did observe consistently copy number increases of mouse chromosome 6 in the K14E6-induced tumors. Mouse chromosome 6 contains the K-*ras* oncogene, an appealing target for increased gene copy number and expression. Quantitative real-time PCR on three E6 tumors and one E7 tumor trisomic for chromosome 6 did not reveal any increased expression of K-*ras* relative to two E7 tumors disomic for this chromosome. Thus, it appears that overexpression of the K-*ras* oncogene via increased gene dosage does not explain the consistent trisomy 6 in the K14E6-induced tumors. Gains of chromosome 6 also have been observed in skin tumors from Senecar mice (47) and TP-*ras* transgenic mice (46) treated with DMBA and TPA. In the former study, however, they additionally observed H-*ras* mutations and gains of chromosome 7, whereas in the latter, translocations of chromosome 4 were seen, resulting in reduced expression of p16[INK4A]. Our results did not reveal any correlation between H-*ras* mutations and a gain of chromosome 6. We did notice that the expression levels of H-*ras* were lower in those tumor cell lines with homozygous-activating mutations at codon 61, implying that in the presence of a constitutively activated H-*ras*, overexpression of the protein is not required for cell growth deregulation. Therefore, additional analysis will be necessary to identify the selective advantage associated with gains of chromosome 6 in mouse skin epithelial tumors.

HPV infection is observed in ~95% of human cervical cancers and is believed to be the earliest event in the pathway to tumorigenesis (19, 51). Likewise, a gain of the long arm of chromosome 3 (3q) is found in 85% of cervical cancers (52–55). The percentage of cells with this cytogenetic alteration increases with the degree of cellular dysplasia (21) and occurs before transition to overt invasive disease (56, 57). Therefore, we were extremely interested to determine whether the chromosome aberrations we observed in our HPV mouse model system correlate with the gain of chromosome 3q in human cervical cancer. Regions corresponding to human chromosome 3p are found on mouse chromosomes 3, 6, 14, and 17, whereas genes localized to human 3q map to mouse chromosomes 3, 6, 9, and 16. Thus, a subset of genes gained in human cervical cancer also is gained consistently in the skin tumors from mice expressing the HPV-E6 oncogene. Recent studies have examined the activation of telomerase in cervical tumors (58) in response to HPV-E6 expression (59) and as a useful biomarker for the early detection of cervical cancer (57, 60). The RNA component of telomerase (*TERC*) maps to the region of chromosome 3 that is gained in cervical cancer (3q26). However, the orthologous region in the mouse (3F/G) is not gained in any of our skin tumors. One interpretation of this result is that a gain of the *TERC* gene is not necessary for tumorigenesis in the presence of E6 expression and that other genes on mouse chromosome 6 that are orthologous to human 3q are the targets of this chromosome gain. Alternatively, the observed disparity in chromosome aneuploidy may be because of differences between mice and humans or in the affected tissue types (cervical *versus* skin epithelial cells).

Aldaz *et al.* (47, 61) have performed numerous studies leading them

---

[3] Unpublished observations.

to the conclusion that mouse papillomas contain the gain of a few chromosomes, namely 6 and 7, and that diverse degrees of aneuploidy exist at the carcinoma stage. Although our study cannot address the chromosomal changes in papillomas, we are in agreement that carcinomas have differing amounts of aneuploidy. However, this was not a reflection of the viral oncogene expressed because the average CIX for the K14E6 and K14E7 tumors was nearly identical (3.7 and 4.0, respectively). It was also not a reflection of the degree of centrosome aberrations. Although the E7 protein acts on the retinoblastoma susceptibility protein pRb and the E6 protein acts, at least in part, to bind and inactivate the tumor suppressor p53, their effects on centrosome numbers do not appear to be markedly different. More precisely, we conclude that murine keratinocytes expressing either E7 or E6 display centrosome abnormalities well above those observed in normal keratinocytes under similar culture conditions. Thus, both proteins have the ability to disrupt centrosome fidelity and generate chromosomal copy number changes via aberrant mitoses.

However, we cannot conclude based on the random chromosome instability observed in our SKY analysis that one affects chromosome segregation more or less than the other. One particularly interesting result from our analysis is that there was not a direct correlation between the level of centrosome aberrations and the degree of chromosome instability in the tumors. Tm5, for instance, has a rather high level of centrosome aberrations in interphase and metaphase, and yet the SKY analysis indicates that these cells are the most chromosomally stable. Conversely, Tm49 had one of the highest instability indices and yet was not dissimilar with respect to centrosome phenotype from tumors with much lower levels of aneuploidy. Thus, we are unable to draw any direct correlation between the extent of centrosome aberrations and the frequency of chromosomal mis-segregation events.

The fact that our K14E7 tumors contain centrosome abnormalities differs from a previous report indicating that inactivation of *Rb* does not result in an increase in centrosome numbers (13). Duensing *et al.* (9, 62) have demonstrated that E7 and E6 are capable of inducing centrosome aberrations in skin tumors and during the immortalization of oral epithelial cells (14). The latter report reveals that this may be caused directly by E7 expression because inhibition of the Rb pathway via loss of expression of p16^{INK4A} or ectopic expression of cdk4, although resulting in immortalization, did not cause centrosome aberrations (14). Thus, it appears that E7 causes dysregulation of the centrosome cycle through inactivation of another protein either alone or in conjunction with inhibition of Rb function.

Tumors from the K14E7 mice contain exceedingly few clonal cytogenetic aberrations, none of which were observed consistently in the group as a whole. Thus, we are unable to reveal a specific associated causative cytogenetic event during tumor formation in the K14E7 mice. However, carcinomas induced by HPV-16 E6 are distinct from their E7 counterparts because they contain a gain of chromosome 6. Our quantitative PCR results argue against the idea that this specific aneuploidy is selected for during tumorigenesis to increase the copy number, and in turn the expression level, of the K-*ras* oncogene in the absence of E7 induction. In conclusion, it appears that our K14E6 and K14E7 mouse models represent two distinct mechanisms of skin tumorigenesis, both of which are independent of H-*ras* mutations or copy number alterations in the K-*ras* gene.

ACKNOWLEDGMENTS

REFERENCES

1. Zheng, L., and Lee, W. H. The retinoblastoma gene: a prototypic and multifunctional tumor suppressor. Exp. Cell Res., 264: 2–18, 2001.
2. Moll, U. M., and Schramm, L. M. p53—an acrobat in tumorigenesis. Crit. Rev. Oral Biol. Med., 9: 23–37, 1998.
3. Kellogg, D. R., Moritz, M., and Alberts, B. M. The centrosome and cellular organization. Annu. Rev. Biochem., 63: 639–674, 1994.
4. Brinkley, B. R. Managing the centrosome numbers game: from chaos to stability in cancer cell division. Trends Cell Biol., 11: 18–21, 2001.
5. Lingle, W. L., Lutz, W. H., Ingle, J. N., Maihle, N. J., and Salisbury, J. L. Centrosome hypertrophy in human breast tumors: implications for genomic stability and cell polarity. Proc. Natl. Acad. Sci. USA, 95: 2950–2955, 1998.
6. Ghadimi, B. M., Sackett, D. L., Difilippantonio, M. J., Schrock, E., Neumann, T., Jauho, A., Auer, G., and Ried, T. Centrosome amplification and instability occurs exclusively in aneuploid, but not in diploid colorectal cancer cell lines, and correlates with numerical chromosomal aberrations. Genes Chromosomes Cancer, 27: 183–190, 2000.
7. Sato, N., Mizumoto, K., Nakamura, M., Nakamura, K., Kusumoto, M., Niiyama, H., Ogawa, T., and Tanaka, M. Centrosome abnormalities in pancreatic ductal carcinoma. Clin. Cancer Res., 5: 963–970, 1999.
8. Carroll, P. E., Okuda, M., Horn, H. F., Biddinger, P., Stambrook, P. J., Gleich, L. L., Li, Y. Q., Tarapore, P., and Fukasawa, K. Centrosome hyperamplification in human cancer: chromosome instability induced by *p53* mutation and/or Mdm2 overexpression. Oncogene, 18: 1935–1944, 1999.
9. Duensing, S., Lee, L. Y., Duensing, A., Basile, J., Piboonniyom, S., Gonzalez, S., Crum, C. P., and Munger, K. The human papillomavirus type 16 E6 and E7 oncoproteins cooperate to induce mitotic defects and genomic instability by uncoupling centrosome duplication from the cell division cycle. Proc. Natl. Acad. Sci. USA, 97: 10002–10007, 2000.
10. Xu, X., Weaver, Z., Linke, S. P., Li, C., Gotay, J., Wang, X. W., Harris, C. C., Ried, T., and Deng, C. X. Centrosome amplification and a defective G2-M cell cycle checkpoint induce genetic instability in *BRCA1* exon 11 isoform-deficient cells. Mol. Cell, 3: 389–395, 1999.
11. Montagna, C., Andrechek, E. R., Padilla-Nash, H., Muller, W. J., and Ried, T. Centrosome abnormalities, recurring deletions of chromosome 4, and genomic amplification of *HER2/neu* define mouse mammary gland adenocarcinomas induced by mutant *HER2/neu*. Oncogene, 21: 890–898, 2002.
12. Weaver, Z., Montagna, C., Xu, X., Howard, T., Gadina, M., Brodie, S. G., Deng, C. X., and Ried, T. Mammary tumors in mice conditionally mutant for *Brca1* exhibit gross genomic instability and centrosome amplification yet display a recurring distribution of genomic imbalances that is similar to human breast cancer. Oncogene, 21: 5097–5107, 2002.
13. Fukasawa, K., Choi, T., Kuriyama, R., Rulong, S., and Vande Woude, G. F. Abnormal centrosome amplification in the absence of *p53*. Science (Wash. DC), 271: 1744–1747, 1996.
14. Piboonniyom, S. O., Duensing, S., Swilling, N. W., Hasskarl, J., Hinds, P. W., and Munger, K. Abrogation of the retinoblastoma tumor suppressor checkpoint during keratinocyte immortalization is not sufficient for induction of centrosome-mediated genomic instability. Cancer Res., 63: 476–483, 2003.
15. Wang, X. J., Greenhalgh, D. A., Jiang, A., He, D., Zhong, L., Brinkley, B. R., and Roop, D. R. Analysis of centrosome abnormalities and angiogenesis in epidermal-targeted p53172H mutant and *p53*-knockout mice after chemical carcinogenesis: evidence for a gain of function. Mol. Carcinog., 23: 185–192, 1998.
16. Wang, X. J., Greenhalgh, D. A., Jiang, A., He, D., Zhong, L., Medina, D., Brinkley, B. R., and Roop, D. R. Expression of a *p53* mutant in the epidermis of transgenic mice accelerates chemical carcinogenesis. Oncogene, 17: 35–45, 1998.
17. Lambert, P., Pan, H., Pitot, H., Liem, A., Jackson, M., and Griep, A. Epidermal cancer associated with expression of human papillomavirus type 16 E6 and E7 oncogenes in the skin of transgenic mice. Proc. Natl. Acad. Sci. USA, 90: 5583–5587, 1993.
18. zur Hausen, H. Human papillomaviruses in the pathogenesis of anogenital cancer. Virology, 184: 9–13, 1991.
19. Bosch, F. X., Manos, M. M., Munoz, N., Sherman, M., Jansen, A. M., Peto, J., Schiffman, M. H., Moreno, V., Kurman, R., and Shah, K. V. Prevalence of human papillomavirus in cervical cancer: a worldwide perspective. International Biological Study on Cervical Cancer (IBSCC) Study Group. J. Natl. Cancer Inst., 87: 796–802, 1995.
20. Song, S., Liem, A., Miller, J. A., and Lambert, P. F. Human papillomavirus types 16 E6 and E7 contribute differently to carcinogenesis. Virology, 267: 141–150, 2000.
21. Ried, T., Heselmeyer-Haddad, K., Blegen, H., Schrock, E., and Auer, G. Genomic changes defining the genesis, progression, and malignancy potential in solid human tumors: a phenotype/genotype correlation. Genes Chromosomes Cancer, 25: 195–204, 1999.
22. Ried, T., Knutzen, R., Steinbeck, R., Blegen, H., Schrock, E., Heselmeyer, K., du Manoir, S., and Auer, G. Comparative genomic hybridization reveals a specific pattern of chromosomal gains and losses during the genesis of colorectal tumors. Genes Chromosomes Cancer, 15: 234–245, 1996.
23. Bockmuhl, U., Wolf, G., Schmidt, S., Schwendel, A., Jahnke, V., Dietel, M., and Petersen, I. Genomic alterations associated with malignancy in head and neck cancer. Head Neck, 20: 145–151, 1998.

24. Herber, R., Liem, A., Pitot, H., and Lambert, P. F. Squamous epithelial hyperplasia and carcinoma in mice transgenic for the human papillomavirus type 16 E7 oncogene. J. Virol., 70: 1873–1881, 1996.

25. Song, S., Pitot, H. C., and Lambert, P. F. The human papillomavirus type 16 E6 gene alone is sufficient to induce carcinomas in transgenic animals. J. Virol., 73: 5887–5893, 1999.

26. Yuspa, S. H., Lichti, U., Morgan, D., and Hennings, H. Chemical carcinogenesis studies in mouse epidermal cell cultures. Curr. Probl. Dermatol., 10: 171–191, 1980.

27. Liyanage, M., Coleman, A., du Manoir, S., Veldman, T., McCormack, S., Dickson, R. B., Barlow, C., Wynshaw-Boris, A., Janz, S., Wienberg, J., Ferguson-Smith, M. A., Schrock, E., and Ried, T. Multicolour spectral karyotyping of mouse chromosomes. Nat. Genet., 14: 312–315, 1996.

28. Garini, Y., Macville, M., du Manoir, S., Buckwald, R. A., Lavi, M., Katzir, N., Wine, D., Bar-Am, I., Schröck, E., Cabib, D., and Ried, T. Spectral karyotyping. Bioimaging, 4: 65–72, 1996.

29. Davisson, M. T. Rules and guidelines for nomenclature of mouse genes. International Committee on Standardized Genetic Nomenclature for Mice. Gene, 147: 157–160, 1994.

30. Weaver, Z. A., McCormack, S. J., Liyanage, M., du Manoir, S., Coleman, A., Schrock, E., Dickson, R. B., and Ried, T. A recurring pattern of chromosomal aberrations in mammary gland tumors of MMTV-cmyc transgenic mice. Genes Chromosomes Cancer, 25: 251–260, 1999.

31. Telenius, H., Pelmear, A. H., Tunnacliffe, A., Carter, N. P., Behmel, A., Ferguson-Smith, M. A., Nordenskjöld, M., Pfragner, R., and Ponder, B. A. J. Cytogenetic analysis by chromosome painting using DOP-PCR amplified flow sorted chromosomes. Genes Chromosomes Cancer, 4: 267–263, 1992.

32. Liu, M. L., Von Lintig, F. C., Liyanage, M., Shibata, M. A., Jorcyk, C. L., Ried, T., Boss, G. R., and Green, J. E. Amplification of Ki-ras and elevation of MAP kinase activity during mammary tumor progression in C3(1)/SV40 Tag transgenic mice. Oncogene, 17: 2403–2411, 1998.

33. Davies, R., Hicks, R., Crook, T., Morris, J., and Vousden, K. Human papillomavirus type 16 E7 associates with a histone H1 kinase and with p107 through sequences necessary for transformation. J. Virol., 67: 2521–2528, 1993.

34. Dyson, N., Guida, P., McCall, C., and Harlow, E. Adenovirus E1A makes two distinct contacts with the retinoblastoma protein. J. Virol., 66: 4606–4611, 1992.

35. Smith-McCune, K., Kalman, D., Robbins, C., Shivakumar, S., Yuschenkoff, L., and Bishop, J. M. Intranuclear localization of human papillomavirus 16 E7 during transformation and preferential binding of E7 to the Rb family member p130. Proc. Natl. Acad. Sci. U S A, 96: 6999–7004, 1999.

36. McIntyre, M. C., Ruesch, M. N., and Laimins, L. A. Human papillomavirus E7 oncoproteins bind a single form of cyclin E in a complex with cdk2 and p107. Virology, 215: 73–82, 1996.

37. Funk, J. O., Waga, S., Harry, J. B., Espling, E., Stillman, B., and Galloway, D. A. Inhibition of CDK activity and PCNA-dependent DNA replication by p21 is blocked by interaction with the HPV-16 E7 oncoprotein. Genes Dev., 11: 2090–2100, 1997.

38. Jones, D. L., Alani, R. M., and Munger, K. The human papillomavirus E7 oncoprotein can uncouple cellular differentiation and proliferation in human keratinocytes by abrogating p21Cip1-mediated inhibition of cdk2. Genes Dev., 11: 2101–2111, 1997.

39. Morozov, A., Shiyanov, P., Barr, E., Leiden, J. M., and Raychaudhuri, P. Accumulation of human papillomavirus type 16 E7 protein bypasses G1 arrest induced by serum deprivation and by the cell cycle inhibitor p21. J. Virol., 71: 3451–3457, 1997.

40. Zerfass-Thome, K., Zwerschke, W., Mannhardt, B., Tindle, R., Botz, J. W., and Jansen-Durr, P. Inactivation of the cdk inhibitor p27KIP1 by the human papillomavirus type 16 E7 oncoprotein. Oncogene, 13: 2323–2330, 1996.

41. Balmain, A., and Pragnell, I. B. Mouse skin carcinomas induced in vivo by chemical carcinogens have a transforming Harvey-ras oncogene. Nature (Lond.), 303: 72–74, 1983.

42. Quintanilla, M., Brown, K., Ramsden, M., and Balmain, A. Carcinogen-specific mutation and amplification of Ha-ras during mouse skin carcinogenesis. Nature (Lond.), 322: 78–80, 1986.

43. Greenhalgh, D. A., Wang, X. J., Rothnagel, J. A., Eckhardt, J. N., Quintanilla, M. I., Barber, J. L., Bundman, D. S., Longley, M. A., Schlegel, R., and Roop, D. R. Transgenic mice expressing targeted HPV-18 E6 and E7 oncogenes in the epidermis develop verrucous lesions and spontaneous, rasHa-activated papillomas. Cell Growth Differ., 5: 667–675, 1994.

44. Brown, K., Quintanilla, M., Ramsden, M., Kerr, I. B., Young, S., and Balmain, A. v-ras genes from Harvey and BALB murine sarcoma viruses can act as initiators of two-stage mouse skin carcinogenesis. Cell, 46: 447–456, 1986.

45. Bailleul, B., Surani, M. A., White, S., Barton, S. C., Brown, K., Blessing, M., Jorcano, J., and Balmain, A. Skin hyperkeratosis and papilloma formation in transgenic mice expressing a ras oncogene from a suprabasal keratin promoter. Cell, 62: 697–708, 1990.

46. Gause, P. R., Lluria-Prevatt, M., Keith, W. N., Balmain, A., Linardopolous, S., Warneke, J., and Powell, M. B. Chromosomal and genetic alterations of 7, 12-dimethylbenz[a]anthracene-induced melanoma from TP-ras transgenic mice. Mol. Carcinog., 20: 78–87, 1997.

47. Aldaz, C. M., Trono, D., Larcher, F., Slaga, T. J., and Conti, C. J. Sequential trisomization of chromosomes 6 and 7 in mouse skin premalignant lesions. Mol. Carcinog., 2: 22–26, 1989.

48. Bremner, R., and Balmain, A. Genetic changes in skin tumor progression: correlation between presence of a mutant ras gene and loss of heterozygosity on mouse chromosome 7. Cell, 61: 407–417, 1990.

49. Burns, P. A., Bremner, R., and Balmain, A. Genetic changes during mouse skin tumorigenesis. Environ. Health Perspect., 93: 41–44, 1991.

50. Bremner, R., Kemp, C. J., and Balmain, A. Induction of different genetic changes by different classes of chemical carcinogens during progression of mouse skin tumors. Mol. Carcinog., 11: 90–97, 1994.

51. Walboomers, J. M., Jacobs, M. V., Manos, M. M., Bosch, F. X., Kummer, J. A., Shah, K. V., Snijders, P. J., Peto, J., Meijer, C. J., and Munoz, N. Human papillomavirus is a necessary cause of invasive cervical cancer worldwide. J. Pathol., 189: 12–19, 1999.

52. Heselmeyer, K., Macville, M., Schrock, E., Blegen, H., Hellstrom, A. C., Shah, K., Auer, G., and Ried, T. Advanced-stage cervical carcinomas are defined by a recurrent pattern of chromosomal aberrations revealing high genetic instability and a consistent gain of chromosome arm 3q. Genes Chromosomes Cancer, 19: 233–240, 1997.

53. Kirchhoff, M., Rose, H., Petersen, B. L., Maahr, J., Gerdes, T., Lundsteen, C., Bryndorf, T., Kryger-Baggesen, N., Christensen, L., Engelholm, S. A., and Philip, J. Comparative genomic hybridization reveals a recurrent pattern of chromosomal aberrations in severe dysplasia/carcinoma in situ of the cervix and in advanced-stage cervical carcinoma. Genes Chromosomes Cancer, 24: 144–150, 1999.

54. Mian, C., Bancher, D., Kohlberger, P., Kainz, C., Haitel, A., Czerwenka, K., Stani, J., Breitenecker, G., and Wiener, H. Fluorescence in situ hybridization in cervical smears: detection of numerical aberrations of chromosomes 7, 3, and X and relationship to HPV infection. Gynecol. Oncol., 75: 41–46, 1999.

55. Yang, Y. C., Shyong, W. Y., Chang, M. S., Chen, Y. J., Lin, C. H., Huang, Z. D., Wang, Hsu, M. T., and Chen, M. L. Frequent gain of copy number on the long arm of chromosome 3 in human cervical adenocarcinoma. Cancer Genet. Cytogenet., 131: 48–53, 2001.

56. Umayahara, K., Numa, F., Suehiro, Y., Sakata, A., Nawata, S., Ogata, H., Suminami, Y., Sakamoto, M., Sasaki, K., and Kato, H. Comparative genomic hybridization detects genetic alterations during early stages of cervical cancer progression. Genes Chromosomes Cancer, 33: 98–102, 2002.

57. Heselmeyer-Haddad, K., Janz, V., Castle, P. E., Chaudhri, N., White, N., Wilber, K., Morrison, L. E., Auer, G., Burroughs, F. H., Sherman, M. E., and Ried, T. Detection of genomic amplification of the human telomerase gene (TERC) in cytologic specimens as a genetic test for the diagnosis of cervical dysplasia. Am. J. Pathol., 163: 1405–1416, 2003.

58. Reesink-Peters, N., Helder, M. N., Wisman, G. B., Knol, A. J., Koopmans, S., Boezen, H. M., Schuuring, E., Hollema, H., de Vries, E. G., de Jong, S., and van der Zee, A. G. Detection of telomerase, its components, and human papillomavirus in cervical scrapings as a tool for triage in women with cervical dysplasia. J. Clin. Pathol., 56: 31–35, 2003.

59. Veldman, T., Horikawa, I., Barrett, J. C., and Schlegel, R. Transcriptional activation of the telomerase hTERT gene by human papillomavirus type 16 E6 oncoprotein. J. Virol., 75: 4467–4472, 2001.

60. Jarboe, E. A., Liaw, K. L., Thompson, L. C., Heinz, D. E., Baker, P. L., McGregor, J. A., Dunn, T., Woods, J. E., and Shroyer, K. R. Analysis of telomerase as a diagnostic biomarker of cervical dysplasia and carcinoma. Oncogene, 21: 664–673, 2002.

61. Aldaz, C. M., and Conti, C. J. The premalignant nature of mouse skin papillomas: histopathologic, cytogenetic, and biochemical evidence. Carcinog. Compr. Surv., 11: 227–242, 1989.

62. Duensing, S., and Munger, K. The human papillomavirus type 16 e6 and e7 oncoproteins independently induce numerical and structural chromosome instability. Cancer Res., 62: 7075–7082, 2002.